

Cite this: *J. Mater. Chem.*, 2011, **21**, 13159

www.rsc.org/materials

## Fabrication of one dimensional superfine polymer fibers by double-spinning†

Mengmeng Li,<sup>ab</sup> Yun-Ze Long,<sup>\*ac</sup> Dayong Yang,<sup>d</sup> Jiashu Sun,<sup>b</sup> Hongxing Yin,<sup>a</sup> Zhili Zhao,<sup>a</sup> Wenhao Kong,<sup>a</sup> Xingyu Jiang<sup>\*b</sup> and Zhiyong Fan<sup>c</sup>

Received 20th May 2011, Accepted 15th July 2011

DOI: 10.1039/c1jm12240a

**We report on a novel spinning technique, termed double-spinning (DS) by combining electro-spinning (ES) and centrifuge-spinning (CS), to fabricate superfine polymer fibers. With a low operating voltage and a slow rotating speed, DS can generate excellent aligned fibrous arrays and two-layer grids with different angles.**

Electro-spinning (ES) is a simple and versatile technique for fabricating uniform ultrafine fibers with diameters ranging from several micrometres down to a few nanometres. In the process of conventional ES, a thin charged jet is formed when the electrostatic force generated by a high operating voltage overcomes the surface tension of the polymer droplet. The jet is accelerated toward the grounded collector and produces fibers in the form of a nonwoven mat. The operating voltages for ES usually range from 10 to 30 kV and the distance between the electrodes is 10–30 cm. In recent years, researchers have demonstrated that ES is a promising method for fabricating micro/nanofibers/tubes<sup>1,2</sup>/spheres<sup>3</sup>/cups<sup>4</sup>/cages<sup>5</sup> from a variety of materials including polymers, ceramics, and even biomacromolecules.<sup>6–10</sup> Among these, ES fibers are being developed as a good potential candidate in many fields, such as tissue engineering, drug release, nano-sensors, energy applications, biochips, and catalyst supports.<sup>11–19</sup> Despite the popularity of the conventional ES, there exist two factors limiting its applications: (1) the random orientation of fibrous mats and (2) the relatively high operating voltage of the ES process. To modify the orientation of fibrous mats, several strategies such as patterning paired electrodes<sup>20,21</sup> and combining magnetic field<sup>22</sup> have been developed to generate fiber based arrays and grid-patterns that can be implemented in high-performance logic circuits, sensors and detectors.<sup>20,22–26</sup> Novel approaches including near-field ES with a small electrode-to-collector distance and high-speed rotary jet-spinning have also been explored to lower or even remove the high

operating voltage.<sup>27,28</sup> Nevertheless, the challenge of controlling the orientation of ES fibers at a relatively low voltage with a simple experimental setup still exists. Herein we report a novel and feasible spinning method to tackle the limitations of conventional ES, achieving highly ordered arrays and grid-patterns with an operating voltage of less than 3 kV. In this new spinning method, we combine conventional ES and centrifuge-spinning (CS) that is also a useful fiber-forming processing technology in order to fabricate superfine fibers. We term this new method double-spinning (DS). In DS, the combination of electrostatic and centrifugal forces stretches polymer solution into fibers, allowing a low operating voltage and a slow rotating speed compared with ES and CS. Notably, DS is capable of producing fibrous arrays with excellent orientation over a large area (more than 2.5 cm × 2.5 cm). In addition, two-layer grid-patterns with different rotation angles 45°, 60° and 90° are also fabricated using DS.

The illustration of the apparatus for DS is shown in Scheme 1. In DS set-up, a syringe with a right-angle stainless needle was fixed horizontally on a circular platform termed “support disk”. This disk was attached to a speed-adjustable motor through an insulated axis, and the rotating radius of the needle was 16 cm. A concentric donut-shaped aluminium foil (inner diameter 20 cm and outer diameter 44 cm) was located under the support disk as the collector. A high-voltage DC power supply (Tianjin Dongwen) was employed to generate required voltages. Using conducting wires, we connected the needle with the anode, and the collector with the cathode. The distance between the tip of the needle and the collector was 5 cm. The rotary motor and the power supply were used to generate the centrifugal force and the electrostatic force on the polymer solution droplet at the orifice of the needle. When the combination of the centrifugal and electrostatic forces exceeded the surface tension of the droplet, a charged polymer jet was ejected from the orifice and accelerated to the collector. As the solvent evaporated, the jet was stretched continually and dramatically decreased in size before it deposited on the collector to produce fibers. During DS, both the right-angle needle and the donut-shaped collector were employed to assist the fiber collection. The CS experiments in our work were carried out by the same DS set-up without the application of the power supply. All the spinning experiments including DS, ES, and CS were conducted at room temperature.

In order to evaluate the three spinning methods (ES, CS and DS), we first produced fibers from the same polymer, polystyrene (PS, Aldrich, average molecular weight of 230 000). Fig. 1a shows

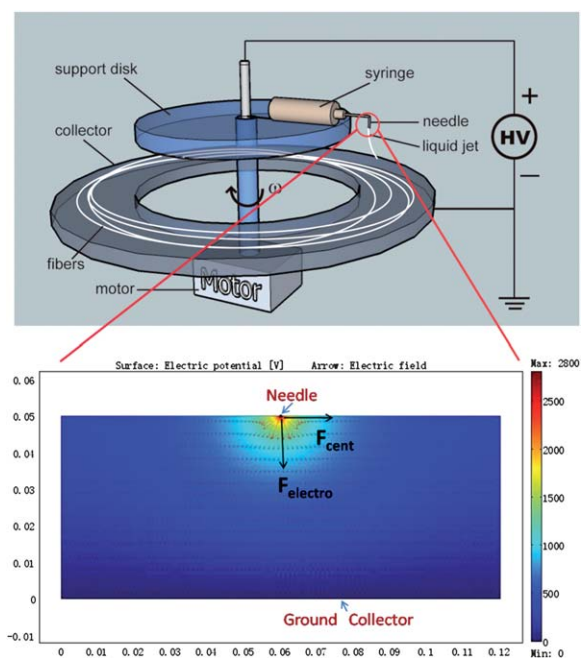
<sup>a</sup>College of Physics Science, Qingdao University, Qingdao, 266071, PR China. E-mail: yunze.long@163.com; Fax: +86-532-8595-5977; Tel: +86-139-5329-0681

<sup>b</sup>National Center for NanoScience & Technology, Beijing, 100190, PR China. E-mail: xingyujiang@nanoctr.cn; Fax: +86-10-8254-5631; Tel: +86-10-8254-5558

<sup>c</sup>Hong Kong University of Science & Technology, Hong Kong, SAR, PR China

<sup>d</sup>Department of Biological and Environmental Engineering, Cornell University, Ithaca, 14850, USA

† Electronic supplementary information (ESI) available. See DOI: 10.1039/c1jm12240a



**Scheme 1** Illustration of the apparatus for double-spinning (DS) to fabricate superfine polymer fibers. The bottom image is the numerical simulation of electric potential (surface) and electric field (red arrows) between the needle and the ground collector. The electrostatic force ( $F_{electro}$ ) and the centrifugal force ( $F_{cent}$ ) were generated by the electric field and the rotary motor, respectively.

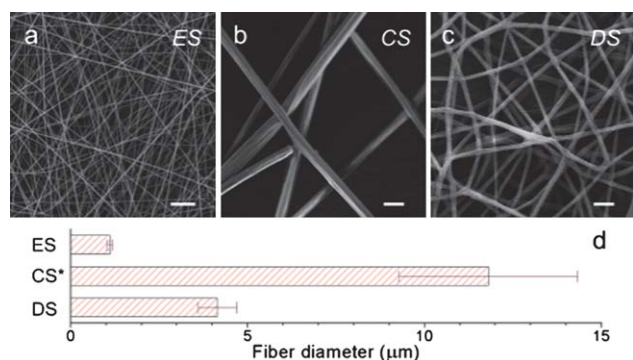


**Fig. 1** (a–c) SEM images of as-spun PS fibers fabricated by electrospinning (ES, 20 kV), centrifuge-spinning (CS, 1200 rpm), and double-spinning (DS, 8.0 kV and 390 rpm). Scale bars are 20 μm. (d) The average diameters of the fibers spun by three methods. \* Do not include the size of the bead structures among CS fibers.

a scanning electron microscopy (SEM, JEOL JSM-6390) image of the continuous uniform fibers with diameters of  $1.10 \pm 0.08 \mu\text{m}$  produced by conventional ES. Though CS can also be used to fabricate long fibers by introducing the centrifugal force, the diameters of the resultant fibers are up to  $11.80 \pm 2.52 \mu\text{m}$ , one order of magnitude larger than those prepared by ES, as shown in Fig. 1b and d. Besides, some bead structures are sometimes observed among CS fibers. The fibers produced by DS are long and fine with diameters of  $4.14 \pm 0.55 \mu\text{m}$ . This number is larger than ES but smaller than CS (see Fig. 1). Nevertheless, compared with a high operating voltage of 20 kV in ES and a fast rotating speed of 1200 rpm in CS, the DS

approach is unprecedented because of the lower applied voltage (8.0 kV) and the slower rotating speed (390 rpm).

We found that the morphologies of DS fibers were strongly dependent on the applied voltage and the rotating speed, so we carried out two groups of experiments in order to characterize these two main factors. First, we varied the applied voltages from 8.0 down to 2.8 kV, with the same rotating speed of 390 rpm, as shown in Fig. 2a. In conventional ES, a lower voltage of less than 5 kV usually results in bad morphologies of spun fibers, and even the failure of spinning. However, Fig. 2c exhibits no significant difference on fiber diameters as operating voltages increase from 2.8 to 8.0 kV by DS. In addition, it is worthy of attention that as the operating voltage decreases, the orientation of DS fibers tends to be aligned along the tangent direction of the support disk. With an operating voltage of 2.8 kV, we can fabricate the uniaxially aligned arrays, whereas when the applied voltage is less than 2.8 kV, the failure of spinning occurs because the total force exerted on the droplet is not strong enough to overcome the surface tension.

Fig. 2b shows the second group of experiments in which we varied the rotation speed from 390 (1<sup>st</sup> image of Fig. 2a) to 870 rpm as the operating voltage was fixed to be 2.8 kV. It has been observed that increasing the rotating speed would greatly reduce the DS fiber alignments. Meanwhile, high rotation speed such as 870 rpm also results in thicker fibers with broad size distribution besides worse fiber alignments, as shown in Fig. 2d. When the rotating speed exceeds 870 rpm, the morphology of bead structures can be observed on the DS fibers. In DS, apart from generating a centrifugal force, another role of rotation is to squeeze the polymer solution from the needle, just like that of the pump in ES, which controls the flow rate of the

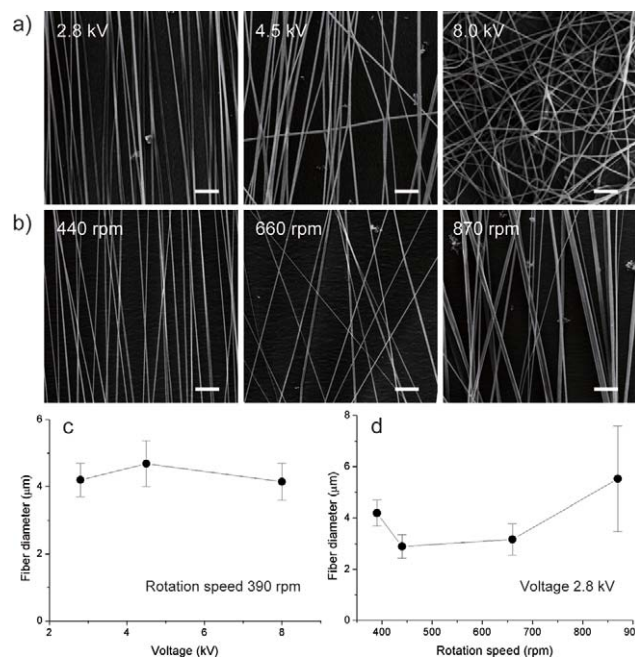


**Fig. 2** Influences of the applied voltage (a, from 8.0 kV to 2.8 kV, the rotating speed is fixed to be 390 rpm) and rotating speed (b, from 440 rpm to 870 rpm, the operating voltage is fixed to be 2.8 kV) on the morphologies of the DS fibers. Scale bars are 50 μm. (c–d) Fiber diameter as a function of the applied voltages and rotation speed. The other experimental parameters are: PS concentration 18%, work distance 5 cm, work radius 16 cm, and DS time 4 min.

solution. High flow rate causes the increase in fibers' diameter and even the appearance of bead morphologies due to the inability of fibers to dry completely before reaching the collector.<sup>29,30</sup> Therefore, we prepared thicker fibers and even bead morphologies with fast rotating speed in our case. In addition, just like the first experiment, too low speed (less than 390 rpm and 2.8 kV) cannot generate enough forces to overcome the surface tension, resulting in poor fabricated fibers or microspheres on the collector. In contrast to the conditions of low applied voltage and speed, the randomly oriented ribbon-shaped fibers that are more than 10  $\mu\text{m}$  in diameter can be obtained with the applied voltages of 15 kV and a rotating speed of 1170 rpm. In addition, polymer concentration in spinning solution is also a critical parameter that greatly influences the morphologies of DS products, as shown in Table S1†. Too low concentration, such as 6% PS, causes the appearance of microspheres and beaded fibers. Nevertheless, spinning fails as the concentration is up to 24%.

Usually, ES utilizes a high applied voltage ranging from 10 to 30 kV to generate the electrostatic force that breaks the balance on the droplet's surface and consequently forms the charged jet. In comparison, DS employs both the electrostatic and centrifugal forces to overcome the surface tension and thus dramatically reduces the operating voltage (2.8 kV in our case). Similarly, due to the application of electric field, a slow rotation speed (390 rpm) is adequate for generating DS fibers. Moreover, the ability to fabricate an aligned fibrous array is another salient advantage of DS. The experimental data suggest that the optimum operating parameters to generate well-aligned DS fibers are 2.8 kV and 390 rpm, respectively, as shown in Fig. 2. During DS, the perpendicular velocity in ES originated from the high electric field is at the magnitude of  $10^0 \text{ m s}^{-1}$  when the polymer jets/fibers close towards the collector.<sup>31,32</sup> And the linear velocity of the needle tip is around  $6.5 \text{ m s}^{-1}$  with a rotation speed of 390 rpm ( $v = \omega r = 2\pi r n = 2 \times 3.14 \times 0.16 \text{ m} \times 390/60 \text{ s} = 6.5 \text{ m s}^{-1}$ ). It has been observed that polymer fibers tend to be aligned when the perpendicular and linear velocities are at the same order of magnitude. Furthermore, once a charged fiber is deposited onto the surface of the collector, a repulsive force originated from Coulomb interactions will influence the next deposited fiber and further improve the fiber alignment.<sup>33</sup>

Fig. 3a and b show the optical and SEM images of the parallel aligned DS fibers respectively. DS is also capable of fabricating fibrous arrays over large areas (more than  $2.5 \text{ cm} \times 2.5 \text{ cm}$ ) with excellent orientation. We measured the angles of orientation ( $\phi$ ) of more than 700 fibers produced using the optimal parameters (2.8 kV and 390 rpm) and quantified the degree of alignment ( $\theta$ ) by comparing  $\phi$  and the long axis (see Fig. S1†). We found that more than 95.5% of the fibers are within  $\theta = 5^\circ$ , and all of the rest are still within  $\theta = 10^\circ$ . If we define  $\alpha$  as the percentage of fibers with  $\theta < 5^\circ$ , DS can produce well aligned fibers with  $\alpha = 95.5 \pm 2.9\%$ . In addition to the operating voltage and the rotation speed, prolonging the spinning time may also influence the alignment of fibers, which can be attributed to the interaction between charged fibers deposited on the collector. However, after collected for 8 min, the majority of fibers are still well aligned with  $\alpha = 89.2 \pm 3.5\%$  (shown in Fig. S2†). Compared with nonwoven mats, aligned fibrous arrays possess much better mechanical properties (see Fig. S3†): their Young's modulus and yield stress are two and three orders of magnitude larger than those of nonwoven mats separately. But their break strain is fairly small.

To build more complex structures such as crossbar junctions, we employed two-step spinning (rotate substrate after the collection of

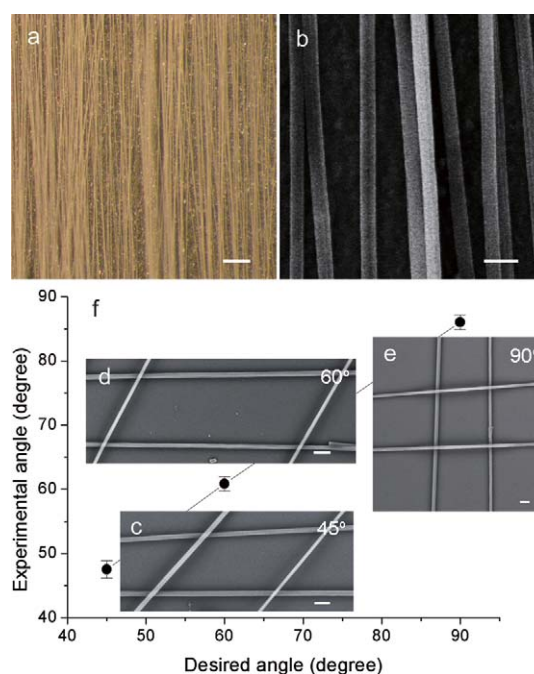


**Fig. 3** a) Optical and (b) SEM images of the DS aligned fibers. (c–e) SEM images of the two-layer grids with different rotation angles: (c)  $45^\circ$ , (d)  $60^\circ$ , and (e)  $90^\circ$ . Scale bars are 200  $\mu\text{m}$  (a) and 10  $\mu\text{m}$  (b–e) respectively. (f) The plots of desired angle versus experimental angle.

the first layer, and then spin again) and deposited fibers onto the same substrate from different angles.<sup>22</sup> Fig. 3c–e exhibit the two-layer grids with different rotation angles of  $45^\circ$ ,  $60^\circ$ , and  $90^\circ$  generated by the two-step spinning, and Fig. 3f reveals that the measured angles between fibers in different layers agree well with the rotation angles. These ordered architectures hold great promise for building complex electronic devices.

As proof-of-principle, we also fabricated DS fibers from other polymers, such as poly(methyl methacrylate) (PMMA, Aldrich, average molecular weight of 350 000). Fig. S4a† shows the SEM image of uniform PMMA fibers with diameters of  $988 \pm 175 \text{ nm}$  in the form of a nonwoven mat using a high operating voltage of 20 kV during ES. When the rotation speed was more than 1000 rpm during CS, the size of the beaded CS fibers was  $6.43 \pm 2.68 \mu\text{m}$  (not including the bead size) (see Fig. S4b†). In comparison, well-aligned PMMA fibers with diameters of  $4.15 \pm 1.07 \mu\text{m}$  were obtained *via* the combination of a lower operating voltage (3 kV) and a slower rotation speed (390 rpm) during DS (see Fig. S4c†). Besides PMMA, poly(vinyl pyrrolidone) (PVP, Aladdin, average molecular weight of 1 300 000) is another common polymer for spinning. When using ethanol as the solvent, we can produce an excellent aligned fibrous array by the DS technique. However, no fibers are formed by spinning PVP/H<sub>2</sub>O solution (see Table S2†). There are at least two key points which can be responsible for this phenomenon: (1) the surface tensions of PVP in different solvents are varied;<sup>29,34–36</sup> (2) the volatilization rate of ethanol is much more rapid than that of water, which is critical in the process of fibers' formation during DS.<sup>30</sup>

In summary, we have developed a novel double-spinning technique for fabricating superfine polymer fibers by combining electro-spinning and centrifuge-spinning. This technique required only a low operating voltage (2.8–3 kV) and a slow rotating speed (390 rpm) to produce polymer fibers, dramatically decreasing the operating

voltage and rotation speed by one order of magnitude in comparison with conventional ES (generally  $\sim 10$  to 30 kV) and CS (generally  $\sim 3000$  to 8000 rpm). Moreover, the DS approach has proved to be effective in preparing fibrous arrays with excellent orientation and fabricating two-layer grids with different angles. In addition, because of the low operating voltage and the slow rotation speed, the proposed DS is expected to be a much safer and more accessible method of producing one dimensional superfine polymer fibers as compared to conventional ES, CS, and other modified ES techniques such as magnetic ES and patterned electrode-collected ES.

## Acknowledgements

We thank Prof. Zhong Zhang, Prof. Luqi Liu, and Yun Gao for their help on the mechanical properties. Prof. Yunze Long acknowledges the financial support of the National Natural Science Foundation of China (grant nos 11074138, 10910101081 and 10604038) and the Program for New Century Excellent Talents in University of China (grant no. NCET-07-0472). Prof. Xingyu Jiang acknowledges the financial support of the Human Frontier Science Program, the National Science Foundation of China (grant nos 90813032, 20890020 and 50902025), the Ministry of Science and Technology (2009CB930001, 2011CB933201, and 2007CB714502), and the Chinese Academy of Sciences (KJCX2-YW-M15).

## Notes and references

- 1 D. Li and Y. N. Xia, *Nano Lett.*, 2004, **4**, 933–938.
- 2 Y. Zhao, X. Y. Cao and L. Jiang, *J. Am. Chem. Soc.*, 2007, **129**, 764–765.
- 3 D. Fantini, M. Zanetti and L. Costa, *Macromol. Rapid Commun.*, 2006, **27**, 2038–2042.
- 4 J. Liu and S. Kumar, *Polymer*, 2005, **46**, 3211–3214.
- 5 Y. Zhu, D. Yang and H. Ma, *Nanoscale*, 2010, **2**, 910–912.
- 6 M. G. McKee, J. M. Layman, M. P. Cashion and T. E. Long, *Science*, 2006, **311**, 353–355.
- 7 M. Li, D. Yang, Y. Long and H. Ma, *Nanoscale*, 2010, **2**, 218–221.
- 8 Y. Liu, D. Yang, T. Yu and X. Jiang, *Electrophoresis*, 2009, **30**, 3269–3275.
- 9 W. Chen, S. He, W. Pan, Y. Jin, W. Zhang and X. Jiang, *Chem. Mater.*, 2010, **22**, 6212–6214.
- 10 Y.-Z. Long, M.-M. Li, C. Gu, M. Wan, J.-L. Duvail, Z. Liu and Z. Fan, *Prog. Polym. Sci.*, 2011, **36**, 1415–1442.
- 11 X. Liu, D. Yang, G. Jin and H. Ma, *J. Mater. Chem.*, 2010, **20**, 10228–10233.
- 12 D. Yang, X. Liu, Y. Jin, Y. Zhu, D. Zeng, X. Jiang and H. Ma, *Biomacromolecules*, 2009, **10**, 3335–3340.
- 13 D. Y. Yang, X. Niu, Y. Y. Liu, Y. Wang, X. Gu, L. S. Song, R. Zhao, L. Y. Ma, Y. M. Shao and X. Y. Jiang, *Adv. Mater.*, 2008, **20**, 4770–4775.
- 14 C. Y. Xu, R. Inai, M. Kotaki and S. Ramakrishna, *Biomaterials*, 2004, **25**, 877–886.
- 15 M. R. Abidian, D. H. Kim and D. C. Martin, *Adv. Mater.*, 2006, **18**, 405–409.
- 16 Z. Y. Li, H. N. Zhang, W. Zheng, W. Wang, H. M. Huang, C. Wang, A. G. MacDiarmid and Y. Wei, *J. Am. Chem. Soc.*, 2008, **130**, 5036–5037.
- 17 A. R. S. Priya, A. Subramania, Y. S. Jung and K. J. Kim, *Langmuir*, 2008, **24**, 9816–9819.
- 18 E. Formo, E. Lee, D. Campbell and Y. N. Xia, *Nano Lett.*, 2008, **8**, 668–672.
- 19 W. Zheng, W. Zhang and X. Jiang, *Adv. Eng. Mater.*, 2010, **12**, B451–B466.
- 20 D. Li, Y. Wang and Y. Xia, *Nano Lett.*, 2003, **3**, 1167–1171.
- 21 D. Li, G. Ouyang, J. T. McCann and Y. N. Xia, *Nano Lett.*, 2005, **5**, 913–916.
- 22 D. Y. Yang, B. Lu, Y. Zhao and X. Y. Jiang, *Adv. Mater.*, 2007, **19**, 3702–3706.
- 23 P. Katta, M. Alessandro, R. D. Ramsier and G. G. Chase, *Nano Lett.*, 2004, **4**, 2215–2218.
- 24 E. Zussman, A. Theron and A. L. Yarin, *Appl. Phys. Lett.*, 2003, **82**, 973–975.
- 25 D. Li, Y. L. Wang and Y. N. Xia, *Adv. Mater.*, 2004, **16**, 361–366.
- 26 Y. Q. Wu, L. A. Carnell and R. L. Clark, *Polymer*, 2007, **48**, 5653–5661.
- 27 D. H. Sun, C. Chang, S. Li and L. W. Lin, *Nano Lett.*, 2006, **6**, 839–842.
- 28 M. R. Badrossamay, H. A. McIlwee, J. A. Goss and K. K. Parker, *Nano Lett.*, 2010, **10**, 2257–2261.
- 29 N. Bhardwaj and S. C. Kundu, *Biotechnol. Adv.*, 2010, **28**, 325–347.
- 30 T. J. Sill and H. A. von Recum, *Biomaterials*, 2008, **29**, 1989–2006.
- 31 D. H. Reneker and A. L. Yarin, *Polymer*, 2008, **49**, 2387–2425.
- 32 D. H. Reneker, A. L. Yarin, H. Fong and S. Koombhongse, *J. Appl. Phys.*, 2000, **87**, 4531–4547.
- 33 B. Sundaray, V. Subramanian, T. S. Natarajan, R. Z. Xiang, C. C. Chang and W. S. Fann, *Appl. Phys. Lett.*, 2004, **84**, 1222–1224.
- 34 H. Liu and Y.-L. Hsieh, *J. Polym. Sci., Part B: Polym. Phys.*, 2002, **40**, 2119–2129.
- 35 H. Fong and D. H. Reneker, *J. Polym. Sci., Part B: Polym. Phys.*, 1999, **37**, 3488–3493.
- 36 Z.-M. Huang, Y. Z. Zhang, M. Kotaki and S. Ramakrishna, *Compos. Sci. Technol.*, 2003, **63**, 2223–2253.